

Degradation of Aramid Fibers Under Alkaline and Neutral Conditions: Relations Between the Chemical Characteristics and Mechanical Properties

G. Derombise,¹ L. Vouyovitch Van Schoors,¹ P. Davies²

¹Division of Material Physicochemistry, Laboratoire Central des Ponts et Chaussées, Paris, France

²Technology Research Department, French Ocean Research Institute, Brest, France

Received 31 March 2009; accepted 4 July 2009

DOI 10.1002/app.31145

Published online 20 January 2010 in Wiley InterScience (www.interscience.wiley.com).

ABSTRACT: Aramid fibers are high-performance materials that have been used in various applications such as heat and cut protection, composites, rubber reinforcement, ropes and cables, and fabrics; today their use is proposed in geotextiles for alkaline ground reinforcement, and they have been used in cables for marine applications for a few years. However, there is a lack of experience with the long-term behavior of aramid fibers in wet and alkaline environments. Aging studies were therefore performed on Twaron 1000 fibers under different conditions (sea water, deionized water, pH 9, and pH 11). Hydrolytic degradation was evaluated with Fourier transform infrared and

viscosimetry measurements, which were correlated with tensile test measurements. The tensile strength followed a logarithmic evolution with the aging time, whereas the modulus remained constant. A linear relation between the tensile strength and the reduced viscosity of the hydrolytically aged fibers is highlighted. Aging indicators are proposed that allow the hydrolytic degradation to be quantified. © 2010 Wiley Periodicals, Inc. *J Appl Polym Sci* 116: 2504–2514, 2010

Key words: ageing; degradation; fibers; structure-property relations; viscosity

INTRODUCTION

Twaron 1000 fibers, produced by Teijin Aramid (Arnhem, The Netherlands), are high-performance fibers based on poly(*p*-phenylene terephthalamide) (PPTA; Fig. 1), and they are similar to Kevlar fibers.¹

The high tensile modulus and tensile strength^{1–7} of PPTA fibers, combined with good chemical resistance in most organic solvents and aqueous salt solutions^{1,2} and a low density,⁷ make them an interesting option for civil engineering applications such as geotextiles and for marine uses such as ropes and instrumentation lines. However, their use in soil reinforcement applications is quite recent.^{8,9} They are being considered as potential replacements for poly(ethylene terephthalate) geotextiles, which display premature aging in alkaline ground (e.g., lime-treated ground or hardened concrete).¹⁰ In marine applications, there is greater experience, up to 30 years,^{2,11} but there are few published data on aging behavior.² This limited experience raises some important durability issues, particularly for civil en-

gineering structures whose required lifetime may be 100 years.

The PPTA hydrolysis mechanism has been identified and involves scission of the amide N–C linkage, which yields acid and amine end functions¹² (Fig. 2).

Several authors have studied the kinetics of hydrolysis of PPTA.^{12,13} For example, Morgan et al.¹² established that the fiber strength degradation (Δ_t) increases with the time, relative humidity (RH), temperature, and applied load:

$$\Delta_t = (RH/100)k_t e^{-(E-K_5\sigma_{\%})/RT} \quad (1)$$

where k_t and K_5 are constants, E is the activation energy for hydrolysis, $\sigma_{\%}$ is the applied stress expressed as a percentage of the fiber strength at time t , R is the gas constant, and T is the absolute temperature. They reported an average strength loss of 0.6% per year for unloaded Kevlar 49 fibers in a 100% RH environment at 23°C and 12% per year at 65°C. Even though the degradation kinetics after sea water exposure have not been studied in detail, some results have been published. For instance, Riewald² reported a 1.5% strength loss for Kevlar 29 and Kevlar 49 yarns after 1 year of immersion. Springer et al.¹³ showed that the addition of 10% NaCl to pure water reduced the tensile strength degradation of Kevlar 49 fibers because of a shielding

Correspondence to: L. Vouyovitch Van Schoors (laetitia.van-schoors@lcpc.fr).

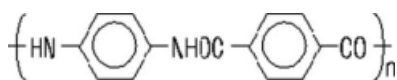


Figure 1 Twaron molecular structure.

effect, whereas it remained unchanged for Twaron 1055 fibers. This latter point has not been explained. The authors also evaluated the mechanical properties of PPTA fibers subjected to aggressive hydrolytic treatments, such as 4 days in H_2SO_4 (40%) at 90°C and in NaOH (10%) at 90°C and 1 day in water at 120°C . The modulus and tensile strength were both affected, but the property drops were larger in acidic and basic solutions than in a neutral environment. The tensile strength evolutions were fitted with the following equation:

$$\sigma = \sigma_0 \left(\alpha_1 \exp \frac{-t}{\tau_1} + \alpha_2 \exp \frac{-t}{\tau_2} \right) \quad (2)$$

where σ is tensile strength at time t and σ_0 is the initial tensile strength, α_1 and α_2 represent the amounts and τ_1 and τ_2 represent the decay times of the two degradation processes. According to the authors, these two processes may be assigned to two different fiber regions (core and shell or crystalline and noncrystalline regions) or to structural elements being stressed differently (loose and taut tie molecules).

The influence of the chain characteristics on the mechanical properties has been examined in previous studies.^{14–17} The theory for the strength of highly oriented liquid crystal polymers developed by Yoon¹⁴ is based on the assumption that the ultimate strength is determined by the strength of intermolecular bonding. It specifies that the tenacity of fully extended, rodlike polymer chains depends on the weight-average molecular mass and its distribution. Termonia and Smith¹⁵ proposed a stochastic model that enabled them to estimate the tensile strength of PPTA fibers as a function of the average molecular weight. They considered the total tensile strain to be governed either by the tensile modulus (primary bonds) or by the shear modulus (secondary hydrogen bonds), depending on the molecular weight. In this way, the authors showed that the tenacity of PPTA fibers with molecular weights ranging from 10,000 to 100,000 g/mol varies approximately as $M^{0.4}$ (where M is the molecular weight). Weyland¹⁶ indicated a linear relation between the inherent viscosity and tenacity of PPTA fibers processed by different methods. In a similar way, North-

olt et al.¹⁷ showed that the sonic modulus and number-average molecular mass are linearly related, using data from different processing experiments: the modulus increases from 87.3 to 99.1 GPa as the number-average molecular weight increases from 11,000 to 15,200 g/mol. The authors explained that the increase in the average chain length may improve the degree of orientation in the domains of the anisotropic solution, and this results in a higher modulus.

These relations between the chain length and tensile properties of PPTA fibers have been established from data based on changing manufacturing conditions. To the best of our knowledge, no similar relation has been confirmed from hydrolytic aging data.

In this study, the hydrolytic degradation of Twaron 1000 fibers immersed in sea and deionized water and in alkaline solutions was evaluated with Fourier transform infrared (FTIR), viscosimetry, and tensile tests. The relationship between the reduced viscosity (related to the weight-average molecular mass) and the mechanical properties was explored.

EXPERIMENTAL

Materials

The Twaron 1000 fiber studied here, in the form of 1680-dtex yarn, is a para-aramid fiber produced by Teijin Aramid.

Aging methods

The fibers were studied in four aging environments. Yarn samples were immersed in buffer sodium carbonate salt solutions at pHs 9 and 11, in deionized water, and in natural sea water. The pH of the buffer solutions was controlled and adjusted every week. The sea water was taken directly from the Brest estuary and filtered to remove biological activity. The pH was measured between 8.04 and 8.57 (at $\sim 14^\circ\text{C}$); the salt concentration was 32.8–33.4 g/L. Deionized water was produced with a Rios water purification system. Four temperatures were considered for each aging condition: 20, 40, 60, and 80°C . Over the aging period considered here, the temperature variability was estimated at $\pm 2^\circ\text{C}$. The deionized water and sea water were circulating and continuously renewed. Aging was also performed in an oven heated at $80 \pm 1^\circ\text{C}$ to evaluate the effect of temperature alone on the fiber characteristics. All aging was performed in total darkness to avoid any UV degradation.

Analysis and characterization

FTIR spectroscopy analysis of the fibers was performed in attenuated total reflectance mode with a

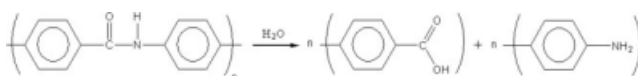


Figure 2 Hydrolysis of PPTA.

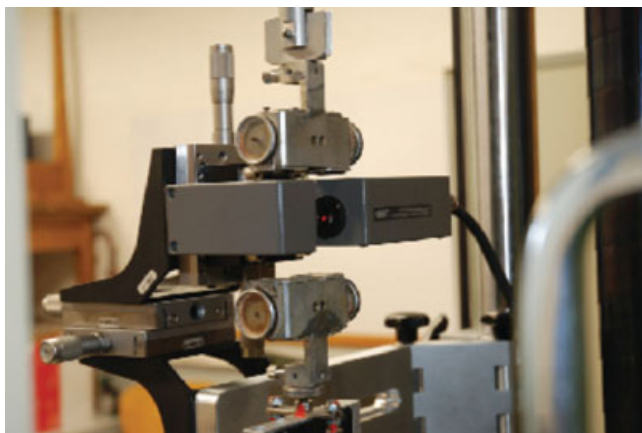


Figure 3 Tensile clamps with a laser micrometer head mounted onto the tensile testing machine. The metal foils are fixed to the tensile clamps. The unitary fiber has been put into a vertical position and adjusted to be perfectly perpendicular to the plane of the laser beam with a three-dimensionally controlled micrometric screw system. [Color figure can be viewed in the online issue, which is available at www.interscience.wiley.com.]

Nicolet Impact 410 spectrometer and a Durascope diamond attenuated total reflectance apparatus. The spectra were recorded with a resolution of 2 cm^{-1} , and there was an accumulation of 32 spectra. The spectra were analyzed with Omnic 3.1 software. Each scan was made with a yarn composed of 1000 filaments and repeated three times per sample and aging condition.

Viscosity measurements were carried out with an Ubbelohde DIN capillary viscosimeter (Schott Instruments) at 25°C . The weight-average molecular mass was calculated from the Mark–Houwink relationship

established by Arpin and Strazielle:¹⁸

$$\eta = 8 \times 10^{-3} M^{1.09}$$

where η is the viscosity and M is the molecular weight. For that purpose, four concentrations between 5×10^{-4} and 2×10^{-3} g/mL were chosen. The reduced viscosity comparisons were performed for the latter concentration. The fibers were dissolved beforehand in sulfuric acid concentrated at 96% for 2 h at 60°C with magnetic stirring. Above this temperature of dissolution, additional degradation can occur in sulfuric acid.¹⁹

The tensile tests were performed on unitary fibers with a Zwick 1474 tensile testing machine with a 5-N force sensor and a rate of extension of 10%/min at 20°C . The fiber diameter, approximately $12\ \mu\text{m}$ on average, was measured before each test with a Mitutoyo LSM-500S laser micrometer (Fig. 3) mounted on the tensile testing machine. The precision of the laser micrometer was $\pm 0.1\ \mu\text{m}$. Around 15 valid measurements were considered for each condition and duration of aging. The tensile modulus was calculated between 0.3 and 0.6% elongation.

RESULTS AND DISCUSSION

The measurements made to follow degradation are of two types: surface measurements (FTIR) and bulk fiber measurements (viscosimetry). These are therefore presented separately. Then, the mechanical properties are described.

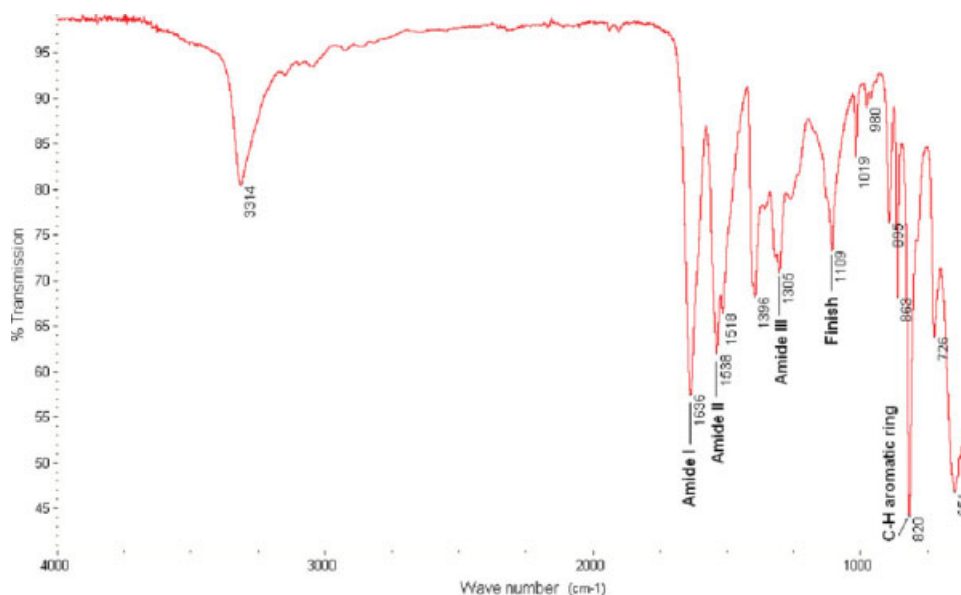


Figure 4 FTIR spectrum of the as-received Twaron 1000 fibers. [Color figure can be viewed in the online issue, which is available at www.interscience.wiley.com.]

TABLE I
Normalized Intensity of the Peaks Related to Amide I of
Twaron 1000 Fibers As Received and After 1 Year of
Aging

	Amide I normalized intensity (%)
As-received	100 ± 1.7
pH 11	
20°C	96.7 ± 1.6
80°C	96.2 ± 0.9
pH 9	
20°C	97.1 ± 3.2
80°C	96.1 ± 0.4
Deionized water	
20°C	96.7 ± 0.9
80°C	96.9 ± 0.6
Sea water	
20°C	97.4 ± 0.4
80°C	94.4 ± 1.2

Evaluation of the degradation at the surface: FTIR

The evolution of the normalized intensity of the peaks related to the amide functions, which are sensitive to hydrolysis, was followed to evaluate the surface degradation of Twaron 1000 fibers. An infrared spectrum of Twaron 1000 as-received fibers is presented in Figure 4.

To perform a semiquantitative analysis, the peaks were normalized with the peak located at approximately 820 cm^{-1} , which was attributed to the C—H deformation of aromatic rings; the intensity appeared to be constant throughout the aging duration. The peaks related to the amide functions were attributed in the following way: the first peak located at approximately 1636 cm^{-1} was related to the C=O vibration (amide I), the second at approximately 1538 cm^{-1} was related to the combined motion of N—H bending and C—N (amide II), and the last at 1305 cm^{-1} was related to combined C—N, N—H, and C—C vibrations (amide III).^{20–22}

Table I presents the evolution of the normalized intensity of a peak related to the amide functions (amide I) for Twaron 1000 fibers after 1 year of aging under different conditions.

It appears that the decrease in the peak related to the amide functions depends neither on the temperature nor on the environment, except in sea water at 80°C; there, the surface degradation is slightly greater. This trend is confirmed in Figure 5, which illustrates the evolution of the amide I peak of Twaron 1000 fibers aged at 80°C under different conditions.

The amide peak evolution curves follow similar trends whatever the aging condition is: the normalized intensity decreases from the beginning of aging and levels off at approximately 7 days and 80°C. The surface hydrolysis is thus a short-term degradation process that tends to equilibrium. At 20°C, the trend is similar for all conditions, but the surface degradation levels off for a longer aging time (after

~41 days). Consequently, the temperature accelerates the surface hydrolysis without affecting the degradation rate after 1 year of aging.

Evaluation of the bulk degradation: viscosity measurements

After the evaluation of the surface degradation of hydrolytically aged Twaron 1000 fibers, the bulk degradation was studied with viscosimetry.

The weight-average molecular mass of the as-received Twaron 1000 fibers was approximately 32,000 g/mol. However, as the reduced viscosity at $2 \times 10^{-3}\text{ g/mL}$ does not require any extrapolation to be calculated, it is used here, as it is a more precise indicator for following low degradation rates.

Figure 6 presents the decrease in the reduced viscosity with the aging time at pH 11, pH 9, in deionized water, and in sea water. From a series of tests of three as-received samples, the precision of the reduced viscosity at $2 \times 10^{-3}\text{ g/mL}$ was estimated to be $\pm 20\text{ mL/g}$.

At pH 11, the reduced viscosity follows a logarithmic evolution with the aging time at 40, 60, and 80°C. The same logarithmic evolution is observed at pH 9, in deionized water, and in sea water at 80°C. For all conditions, it appears that the higher the temperature is, the higher the degradation rate is after 1.5 years of aging. For example, after 1.5 years of aging at pH 11, the reduced viscosity decreases by 64% at 80°C, whereas it decreases by 13% at 20°C. Hydrolysis is thus accelerated by the temperature, as suggested by Morgan et al.¹²

Figure 7 groups the degradation curves of Twaron 1000 fibers in different environments at 80°C.

It appears that the hydrolytic environment has a significant influence on the degradation: the degradation is greater at pH 11 than in sea and deionized

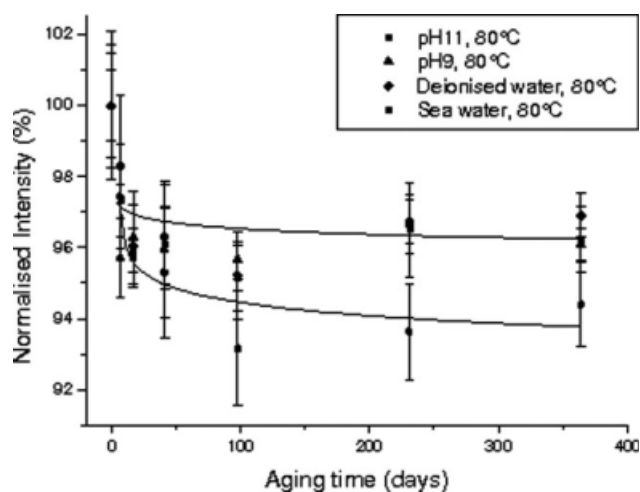


Figure 5 Evolution of the normalized intensity of the peaks related to the amide function (amide I) of hydrolytically aged Twaron 1000 fibers.

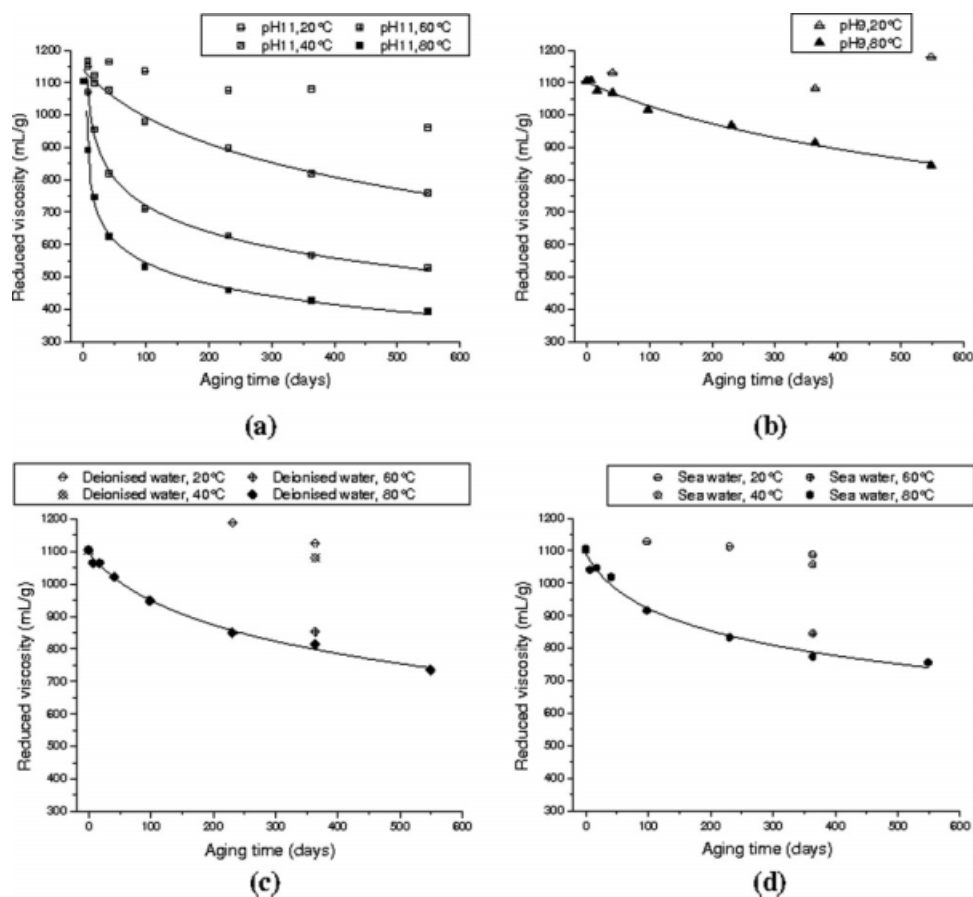


Figure 6 Evolution of the reduced viscosity at 2×10^{-3} g/mL (a) at pH 11, (b) at pH 9, (c) in deionized water, and (d) in sea water.

water and greater in sea and deionized water than at pH 9. The higher degradation rate in deionized and sea water versus that at pH 9 may be explained by an additional reaction occurring under the former conditions. Indeed, a possible hydrolysis of amide groups by acid catalysis could be superimposed on the hydrolysis by basic catalysis. Further work is needed to explain the kinetics. The degradation curves of fibers aged in sea and deionized water are almost superimposed, revealing that the reduced viscosity is not affected by the presence of NaCl salt in the water. The aging in air at 80°C reveals that thermooxidative degradation is not a serious concern for chain degradation.

The previously shown reduced viscosity curves cannot be fitted with eq. (1), which was established by Morgan et al.¹² for tensile strength evolution: the mechanisms involved appear to be different, and the fiber grades studied here are not the same as those in the previous work. Moreover, Morgan et al. established their kinetics for 100% RH exposure, whereas the aging considered here has been performed under immersion. However, the data can be fitted by logarithmic laws and modeled by eq. (2) (to which an additional constant term has been added), which

was established by Springer et al.¹³ for tensile strength evolution.

For Twaron 1000 fibers aged at pH 11 and 80°C, the data are best fitted with two decay functions (with an adjusted coefficient of determination > 0.998); two degradation processes may be thus considered. At pH 9 and 80°C, the data are best fitted with one decay function only (adjusted $R^2 > 0.96$). In a similar way, in sea and deionized water at 80°C, the data are best fitted with one decay function (adjusted $R^2 > 0.982$). This suggests that there may be one predominant degradation process under these aging conditions. The corresponding decay parameters, calculated from Springer et al.'s equation,¹³ are listed in Table II except for aging at pH 9 and 80°C, which yields physically unacceptable parameters.

At pH 11, the two processes have the following characteristics: the first one is predominant and has a relatively short decay time, whereas the second displays a much longer decay time. Wide-angle X-ray scattering measurements of Twaron 1000 fibers aged at pH 11 and at pH 9²³ and in deionized and sea water reveal an increase in the lateral apparent crystallite size (ACS), as observed by Springer

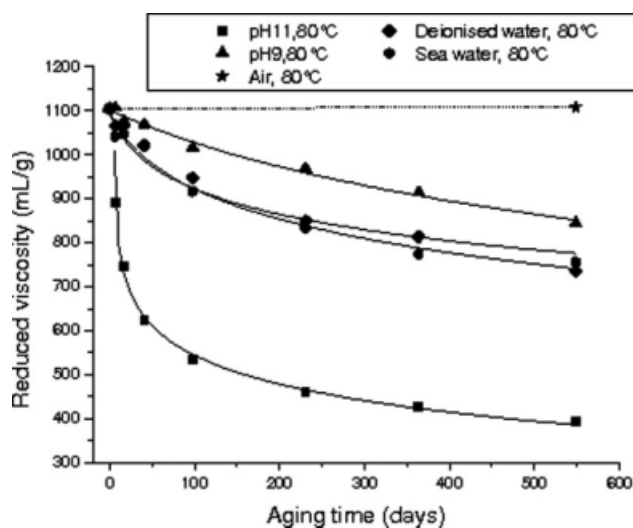


Figure 7 Evolution of the reduced viscosity at 2×10^{-3} g/mL of the Twaron 1000 fibers aged under different conditions at 80°C .

et al.¹³ for Kevlar 49 fibers after different hydrolytic treatments. The latter authors attributed this increase to the recrystallization of degraded tie molecules at the surface of the crystallites. These tie molecules are mentioned in the structural models proposed by Panar et al.²⁴ and Li et al.²⁵ for PPTA fibers. Indeed, Panar et al. suggested that the core of PPTA fibers is composed of periodic crystallites layers linked together in the fiber direction by extended chains passing through two consecutive layers. As Morgan and Pruneda²⁶ suggested that the water molecules preferentially accumulate in the interfibrillar region, the increase in the lateral ACS could also be related to the destruction of the tie fibrils, which, according to Panar et al., ensure the cohesion between adjacent fibrils. Finally, this could be attributed to the degradation of potential imperfectly crystallized chains located at the surface of the crystallites. At pH 9, this degradation, leading to an increase in the lateral ACS, must be the only degradation process that occurs, as only one decay function is needed to fit the data. At pH 11, an additional degradation process has to be considered; for instance, it may be the degradation of the crystallites themselves, which would be a lower rate degradation process as the water molecules do not penetrate the crystallites.²⁷

TABLE II
Weights and Decay Times of Functions Used To Fit the Reduced Viscosity at 2×10^{-3} g/mL for Degradation Curves from eq. (2)

Aging conditions	α_1 (%)	α_2 (%)	τ_1 (days)	τ_2 (days)
pH 11, 80°C	61	39	12	162
Deionized water, 80°C	100	—	230	—
Sea water, 80°C	100	—	157	—

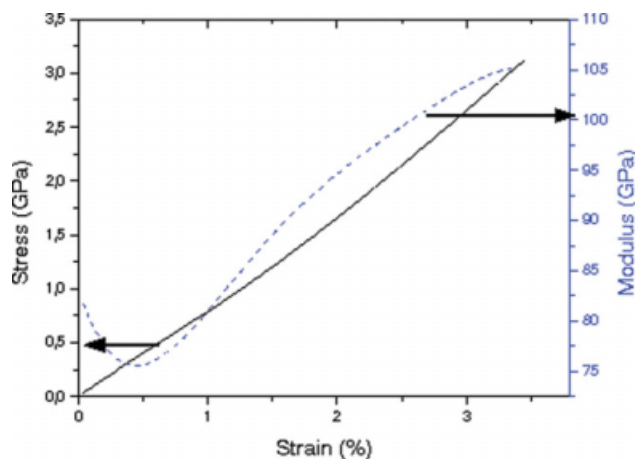


Figure 8 Stress–strain and modulus–strain curves for the as-received Twaron 1000 fibers. [Color figure can be viewed in the online issue, which is available at www.interscience.wiley.com.]

We suggest that hydrolysis may preferentially occur at both ends of the chains, as the amide linkage adjacent to the chain end group is more exposed to hydrolysis.²⁴

Influence of the degradation of the PPTA chains on the tensile properties

Chain scission phenomena have been highlighted both in the core and at the surface of hydrolytically aged Twaron 1000 fibers. The effects of the degradation on the mechanical properties are studied in the following section.

Figure 8 shows a typical stress–strain curve and a modulus–strain curve for the as-received Twaron 1000 fibers.

The modulus curve first decreases with strain to a minimum located around 0.5% strain and then increases up to the tensile break, and this is in accordance with other studies.^{28–30} The modulus of the aged fibers displays exactly the same trend and similar values for a given strain rate up to the tensile break. That is why the modulus can be compared in any strain range; in this study, we have chosen 0.3–0.6%. No significant diameter changes have been noted for any condition or duration of aging; all the diameters range from 11.3 to 12 μm . The initial tensile strength is 3.23 ± 0.45 GPa, and the tensile modulus is 80 ± 11 GPa. However, to avoid any error due to the slight differences measured in the diameters, the tensile properties are expressed in newtons and then normalized.

Yeh and Young⁴ reported that the tensile modulus of different grades of Kevlar and Twaron fibers increases with the strain up to the tensile break. On the basis of studies by Northolt and coworkers,^{31–33} the authors attributed the increase in the modulus to

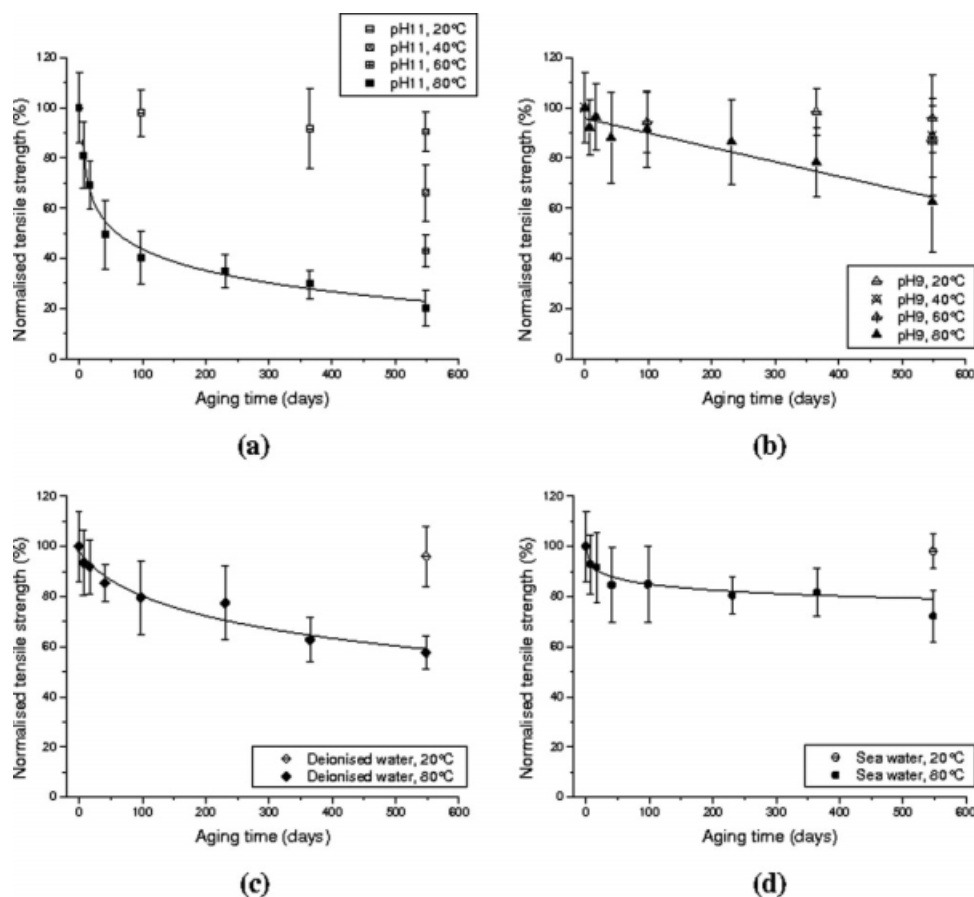


Figure 9 Evolution of the tensile strength with the aging time (a) at pH 11, (b) at pH 9, (c) in deionized water, and (d) in sea water.

an increase in the molecular alignment along the fiber axis during tensile deformation. Our modulus-strain curves display similar behavior, with the exception of an initial decrease in the modulus observed up to approximately 0.5% strain. This initial decrease in the modulus could be explained by hydrogen bonds or tie fibril disruptions before the orientation of the chains toward the fiber axis.

Tensile strength

The tensile strength of Twaron 1000 fibers has been evaluated at different aging times. The evolution curves are presented in Figure 9.

At pH 11 and 80°C and in sea and deionized water at 80°C, the tensile strength degradation follows, to a first approximation, a logarithmic evolution with time. At pH 9 and 80°C, the tensile strength degradation seems to follow a linear evolution, but it could also be a logarithmic evolution, which would not be clearly visible within the accuracy of the measurements. Moreover, for all conditions, the higher the temperature is, the greater the degradation is. It is confirmed, once more, that the degradation is accelerated by the temperature. For

instance, after 7 days at pH 11 and 80°C, the drop in strength is already greater than that after 18 months at 20°C, and this suggests an acceleration factor close to 80. More work is needed to quantify this factor more precisely. Table III reports the residual tensile strength of Twaron 1000 fibers after 1.5 years of aging under different conditions at 80°C.

After 1.5 years at 80°C in air, the strength degradation is close to 8%: thermooxidation is thus not a serious concern for the tensile strength. However, the degradation is significant in wet environments. It appears that the degradation is greater at pH 11 than under the other conditions. After 1.5 years at pH 9 and in deionized water, the degradation in

TABLE III
Residual Tensile Strength of Twaron 1000 Fibers After 1.5 Years of Aging Under Different Conditions

Conditions	Residual tensile strength (%)
As received	100 ± 14
pH 11, 80°C	20 ± 7
pH 9, 80°C	62 ± 20
Deionized water, 80°C	58 ± 7
Sea water, 80°C	72 ± 10
Air, 80°C	92 ± 12

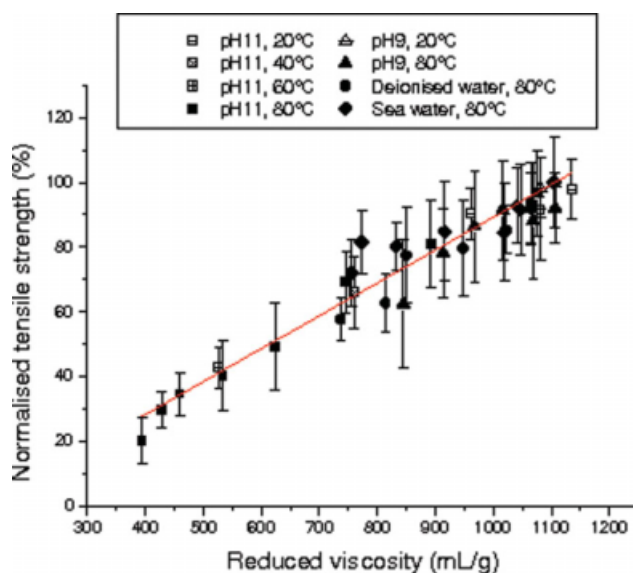


Figure 10 Relation between the reduced viscosity at 2×10^{-3} g/mL and the normalized tensile strength of the Twaron 1000 fibers aged under different conditions. [Color figure can be viewed in the online issue, which is available at www.interscience.wiley.com.]

tensile strength is similar, and it is slightly lower under sea water exposure.

As the tensile strength and the reduced viscosity seem to follow similar evolutions, except at pH 9, these two characteristics must be closely related. Figure 10 plots the reduced viscosity versus the residual tensile strength.

The tensile strength and the reduced viscosity are correlated with a p value of 2.79×10^{-21} . It appears that they can be correlated, to a first approximation, with a linear relationship (adjusted coefficient of determination > 0.934), which is in accordance with results from a previous study.¹⁶ This correlation supports the hypothesis that the tensile strength is governed by the lateral intermolecular bonds, as shown previously by Yoon.¹⁴ It seems unlikely that the dis-

ruption of hydrogen bonds within the crystallites can occur, as the water does not penetrate the crystallites.²⁷ The degradation of interfibrillar lateral bonds, like the tie fibrils mentioned by Panar et al.,²⁴ is a more likely process. This assumption is supported by the increase in the lateral ACS of the hydrolytically aged fibers.²³ The decrease in the tensile strength may also result from the degradation of the tie molecules mentioned by Panar et al. and Li et al.²⁵ Further work is needed to identify the nature of the bonds that are degraded during hydrolysis.

Figure 11(a,b) focuses on the relationship between the tensile strength and the reduced viscosity, respectively, at pHs 11 and 9 and in deionized and sea water.

The slight deviation from the straight line, observed at pH 9 [Fig. 11(a)], may come from additional structural changes occurring under this aging condition. The deviation observed for aging under sea water exposure [Fig. 11(b)] may result from a different degradation mechanism. Indeed, as the surface degradation is slightly greater in sea water than in deionized water and the bulk degradations are similar, it is likely that the core degradation is less important in sea water. The salinity of water would thus limit the water diffusion into the fibers and accelerate the surface degradation. As the residual tensile strength is higher after aging in sea water than in deionized water (this differs from Springer et al.'s results¹³), one might conclude that the core degradation governs the residual strength to a greater extent.

Tensile modulus

Figure 12 shows the evolution of the tensile modulus measured between 0.3 and 0.6% strain with the aging time for all conditions.

The tensile modulus of Twaron 1000 fibers aged under different conditions does not display any sig-

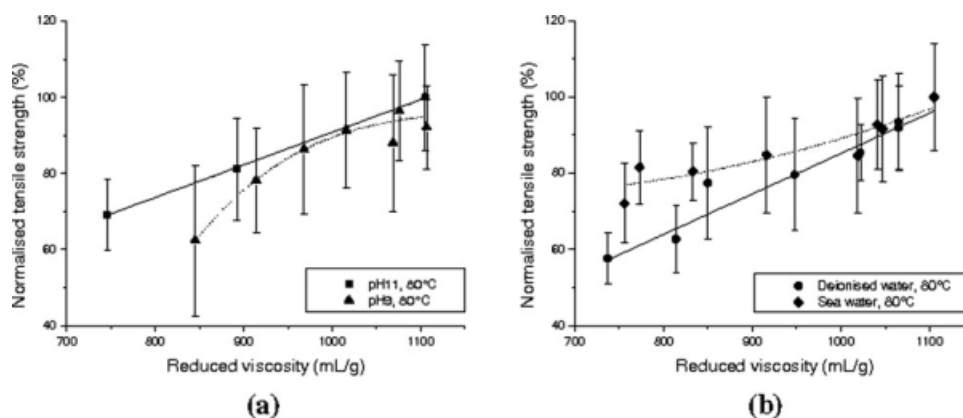


Figure 11 Relation between the reduced viscosity at 2×10^{-3} g/mL and the normalized tensile strength of the Twaron 1000 fibers aged (a) at pH 11 and pH 9 and (b) in deionized water and sea water.

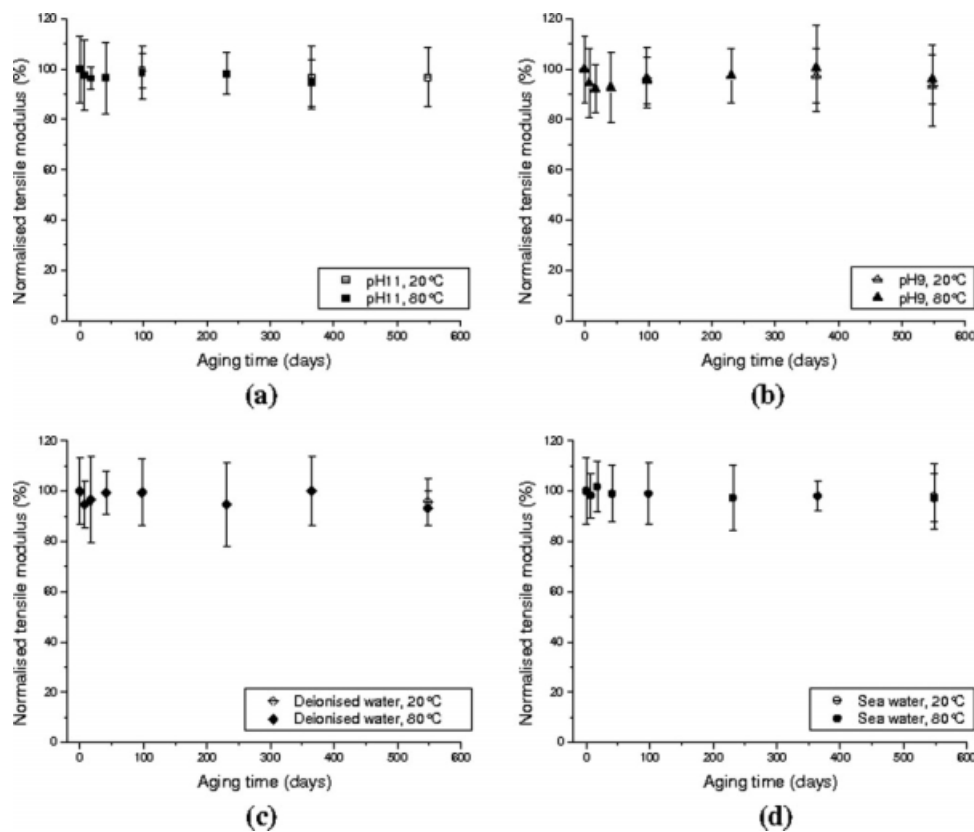


Figure 12 Evolution of the tensile modulus with the aging time (a) at pH 11, (b) at pH 9, (c) in deionized water, and (d) in sea water.

nificant evolution after aging. Even after 1 year at pH 11 and 80°C, the modulus decreases by only approximately 5%, whereas the tensile strength decreases by approximately 70%. Similar trends were observed by Zhang et al.²² for Twaron 2000 aged under UV irradiation: after a 144-h UV exposure, the tenacity drop that they observed was close to 55%, whereas the decrease in the tangent modulus (measured at 0.5% strain) was lower than 10%.

Northolt et al.¹⁷ proposed a relation between the strength and modulus of well-oriented PPTA that is in accordance with their experimental data: the tensile strength increases with the modulus. The experimental data obtained in this study do not show this trend.

To explain this behavior, an analogy with composite materials reinforced by unidirectional long fibers is proposed, as illustrated in Figure 13. The fibrils of PPTA fibers may act as the long fibers of composites, whereas the tie fibrils mentioned by Panar et al.²⁴ may be assimilated to an equivalent matrix material.

In composites, the load transfer between the fibers is ensured by the matrix through shear stresses at the interface. In PPTA fibers, the load transfer between fibrils may occur in the interfibrillar regions via angled tie fibrils, which ensure shear transfer by

tension compression. The disruption of these tie fibrils may thus limit the load transfer between the fibrils. Thus, when the tension stress in a bundle of isolated longitudinal fibrils (that are no longer linked to other fibrils) reaches the strength of the weakest link of the fibrils, the fibrils break and cease to sustain load. Thus, for the same level of loading, the stresses in other fibrils suddenly increase, and this results in a higher probability of failure for these other fibrils. On the contrary, when the tie fibrils are

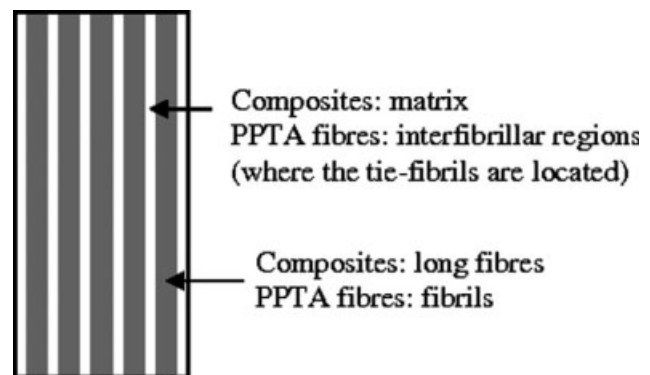


Figure 13 Analogy between the composites reinforced with long fibers and the PPTA fibrillar structure (as described by Panar et al.²⁵).

not damaged, they can play an important role in the redistribution of stresses along the broken fibrils and in the global strength of the fiber. The fragments of broken fibrils may continue to bear the external loading up to a critical size.

Moreover, the degradation of the tie molecules (chains passing through two consecutive crystallites) mentioned by Panar et al.²⁴ and Li et al.²⁵ may generate structural defects that also increase the probability of failure in tension, thus decreasing the fiber tensile strength.

These two phenomena can explain the decrease in the fiber tensile strength.

On the contrary, the tensile modulus of composite materials depends exclusively on the volume fraction of the matrix (V_M) and on the volume fraction of the fibers (V_F) as defined by the rule of mixtures:

$$E_L = V_F E_F + V_M E_M \quad (3)$$

where E_L is the longitudinal modulus of the composite, E_F is the tensile modulus of the fibers, and E_M is the tensile modulus of the matrix.

The connection between the fibers and matrix does not enter into this expression and does not influence the value of the equivalent modulus (E_L). Moreover, here the equivalent modulus (E_M ; i.e., the axial modulus of angled links) is negligible in comparison with E_F .

Consequently, although the degradation of the tie fibrils is very important for the strength of the fiber, it may not induce any change in the longitudinal modulus as the volume fraction of the fibrils and the volume fraction of the interfibrillar regions are conserved during aging.

In addition, as the modulus of PPTA fibers depends on the orientation along the fiber,^{3-5,31-35} it may be concluded that the macromolecular chains retain their initial orientation during hydrolytic aging, despite chain degradation.

CONCLUSIONS

Twaron 1000 fibers have been aged under alkaline conditions (pHs 9 and 11), in natural sea water, and in deionized water. Several conclusions may be proposed:

- Hydrolytic degradation occurs at the surface of the fiber.
- The hydrolytic bulk degradation follows a logarithmic law with time and is accelerated by the temperature.
- The reduced viscosity decrease is larger at pH 11 than in sea and deionized water but larger in sea and deionized water than at pH 9.

- Two degradation processes may be involved at pH 11, and these may be attributed to the degradation of the tie fibrils/molecules and/or imperfectly crystallized chain segments on the one hand and to the degradation of the crystallites on the other hand. Only one degradation process may operate at pH 9, in sea water, and in deionized water: the degradation of the tie fibrils/molecules and/or imperfectly crystallized chain segments.
- A linear correlation can be made between the reduced viscosity and the tensile strength.

The tensile modulus is unchanged even after a 1.5-year aging period. The physicochemical and structural changes involved do not have any influence on the tensile modulus.

This work shows that the reduced viscosity is a useful aging indicator that can be used to predict the remaining strength of Twaron 1000 fibers after hydrolytic degradation. This should enable the long-term durability of these fibers to be quantified. This approach is now being extended to other aramid fibers.

The authors are grateful to Otto Grabandt and Bertil van Berkel of Teijin-Aramid for the fiber samples and their cooperation. The contributions of Nicolas Barberis, Dominique Duragrain (Laboratoire Central des Ponts et Chaussées), and Nicolas Lacotte (French Ocean Research Institute) are also greatly appreciated. Special thanks go to Xavier Colin (Ecole Nationale Supérieure d'Arts et Métiers) and Jean-François Caron (Ecole des Ponts ParisTech) for very rewarding discussions.

References

1. Yang, H. H. *Kevlar Aramid Fibers*; Wiley: New York, 1993.
2. Riewald, P. G. *AIChE Symp Ser* 1980, 76, 133.
3. Dobb, M. G.; Robson, R. M. *J Mater Sci B* 1990, 25, 459.
4. Yeh, W.-Y.; Young, R. J. *Polymer* 1999, 40, 857.
5. Rao, Y.; Waddon, A. J.; Farris, R. J. *Polymer* 2001, 42, 5925.
6. Hindeleh, A. M.; Abdo, S. M. *Polym Commun* 1989, 30, 184.
7. Technora—High Tenacity Fibres; Teijin.
8. Auray, G.; Simons, D. *JEC Compos Mag* 2007, 35, 58.
9. Blivet, J.-C.; Garcin, P.; Hirschauer, A.; Nancey, A.; Villard, P. *Proc Rencontres Géosynth* 2006, 281.
10. Benneton, J.-P.; Blivet, J.-C.; Perrier, H. *Proc Rencontres Géotext Géomembr* 1997, 58.
11. Swenson, R. C. *Proc Offshore Technol Conf* 1983, 3, 467.
12. Morgan, R. J.; Pruneda, C. O.; Butler, N.; Kong, F.-M.; Caley, L.; Moore, R. L. *Proc Natl SAMPE Symp* 1984, 29, 891.
13. Springer, H.; Abu Obaid, A.; Prabawa, A. B.; Hinrichsen, G. *Text Res J* 1998, 68, 588.
14. Yoon, H. N. *Colloid Polym Sci* 1990, 268, 230.
15. Termonia, Y.; Smith, P. *Polymer* 1980, 27, 1845.
16. Weyland, H. G. *Polym Bull* 1980, 3, 331.
17. Northolt, M. G.; den Decker, P.; Picken, S. J.; Baltussen, J. J. M.; Schlattmann, R. *Adv Polym Sci* 2005, 178, 1.
18. Arpin, M.; Strazielle, C. *Polymer* 1977, 18, 591.
19. Aoki, H.; Onogi, Y.; White, J. L.; Fellers, J. F. *Proc Annu Tech Conf Soc Plast Eng* 1979, 37, 642.

20. Penn, L.; Larsen, F. J Appl Polym Sci 1979, 23, 59.
21. Park, S.-J.; Seo, M.-K.; Ma, T.-J.; Lee, D.-R. J Colloid Interface Sci 2002, 252, 249.
22. Zhang, H.; Chen, J.; Hao, X.; Wang, S.; Feng, X.; Guo, Y. Polym Degrad Stab 2006, 91, 2761.
23. Derombise, G.; Vouyovitch Van Schoors, L.; Davies, P. J Mat Sci, Submitted.
24. Panar, M.; Avakian, P.; Blume, R. C.; Gardner, K. H.; Gierke, T. D.; Yang, H. H. J Polym Sci Polym Phys Ed 1983, 21, 1955.
25. Li, L.-S.; Allard, L. F.; Bigelow, W. C. J Macromol Sci Phys 1983, 22, 269.
26. Morgan, R. J.; Pruneda, C. O. Polymer 1987, 28, 340.
27. Fukuda, M.; Ochi, M.; Miyagawa, M.; Kawai, H. Text Res J 1991, 61, 668.
28. Chailleux, E.; Davies, P. Mech Time-Dependent Mater 2003, 7, 291.
29. Allen, S. R.; Roche, E. J. Polymer 1989, 30, 996.
30. Northolt, M. G.; Baltussen, J. J. M.; Schaffers-Korff, B. Polymer 1995, 36, 3485.
31. Northolt, M. G.; van Aartsen, J. J. J Polym Sci Polym Symp 1977, 58, 283.
32. Northolt, M. G. Polymer 1980, 21, 1999.
33. Northolt, M. G.; van der Hout, R. Polymer 1985, 26, 310.
34. Rao, Y.; Waddon, A. J.; Farris, R. J. Polymer 2001, 42, 5937.
35. Lee, K.-G.; Barton, R.; Schultz, J. M. J Polym Sci Part B: Polym Phys 1995, 1, 33.